Formation cross-sections of singlet and triplet excitons in π-conjugated polymers

M. Wohlgenannt*†, Kunj Tandon†‡, S. Mazumdar§, S. Ramasesha‡ & Z. V. Vardeny*

** Department of Physics, University of Utah, Salt Lake City, Utah 84112, USA*
‡ Solid State and Structural Chemistry Unit, Indian Institute of Science, Bangalore 560012, India
§ Department of Physics, University of Arizona, Tucson, Arizona 85721, USA
† These authors contributed equally to this work

Electroluminescence in organic light-emitting diodes arises from a charge-transfer reaction between the injected positive and negative charges by which they combine to form singlet excitons that subsequently decay radiatively. The quantum yield of this process (the number of photons generated per electron or hole injected) is often thought[1] to have a statistical upper limit of 25 per cent. This is based on the assumption that the formation cross-section of singlet excitons, σ_S, is approximately the same as that of any one of the three equivalent non-radiative triplet exciton states, σ_T; that is, $\sigma_S/\sigma_T \approx 1$. However, recent experimental[2] and theoretical[3] work suggests that σ_S/σ_T may be greater than 1. Here we report direct measurements of σ_S/σ_T for a large number of π-conjugated polymers and oligomers. We have found that there exists a strong systematic, but not monotonic, dependence of σ_S/σ_T on the optical gap of the organic materials. We present a detailed physical picture of the charge-transfer reaction for correlated π-electrons, and quantify this process using exact valence bond calculations. The calculated σ_S/σ_T reproduces the experimentally observed trend. The calculations also show that the strong dependence of σ_S/σ_T on the optical gap is a signature of the discrete excitonic energy spectrum, in which higher energy excitonic levels participate in the charge recombination process.

The charge transfer (CT) reaction between the injected spin-half positively and negatively charged polarons (P^+ and P^-) proceeds by an intermediate metastable encounter complex (EC). The EC is a superposition of the overall eigenstate $|I\rangle$ of the initial reactant species and the overall eigenstate $|F\rangle$ of the final products of the CT reaction. Following the formation of an EC, conformational changes along reaction coordinates occur, leading to the formation of $|F\rangle$. For large yields $|\mathrm{EC}\rangle$ must have simultaneously large overlaps with both $|I\rangle$ and $|F\rangle$. Here $|I\rangle = |P^+\rangle|P^-\rangle$, $|F\rangle = |[S/T]\rangle + |G\rangle$, with $|P^\pm\rangle$ being the polaron eigenstates, $|[S/T]\rangle$ is either a neutral singlet or a neutral triplet excited state of one participant, and $|G\rangle$ is the ground state of the other participant. In the absence of electron correlation $|P^\pm\rangle$, $|[S/T]\rangle$ and $|G\rangle$ are all described by single configurations[4]. In particular, as the occupancies of the one-electron levels are the same for the singlet and triplet, $\sigma_S \approx \sigma_T$ for weak electron correlation.

The above description breaks down for intermediate electron correlations that are valid for π-conjugated polymers. First, single-configuration descriptions are no longer valid. The $|P^\pm\rangle$ are now superpositions of multiple configurations involving low (high) energy occupied (unoccupied) one-electron levels. Thus partial CT leads to multiple excited states of the EC supermolecule, each of which can decay to give the neutral states of the two components. Second, the correlated singlet exciton is necessarily ionic, whereas the correlated triplet exciton has a large covalent character[5]; there is also a substantial energy splitting between them[6–8]. For large exciton production, the sum of the overlaps of the different eigenstates $|\mathrm{EC}_j\rangle$ with $|I\rangle$ and $|F\rangle$ must be large. Because the initial polaronic species P^+ and P^- are necessarily ionic, the dominant $|\mathrm{EC}_j\rangle$ must also be ionic, and hence the most likely outcome of the CT reaction is the creation of product species, at least one of which is ionic. We conclude that $\sigma_S > \sigma_T$. Furthermore, the relative contributions of electron correlation and topology to the overall optical gap, which determine the ionicities of the ground and excited states, are strongly material-dependent; hence we expect σ_S/σ_T to be material-dependent from general considerations alone.

For systems which are light-emitting the quantum efficiency for electroluminescence (EL) is $\eta_{EL} = \eta_1\eta_2\eta_3$, where η_1 is the singlet emission quantum efficiency, η_2 is the fraction of the total number of excitons that are singlets, and η_3 is the probability that the injected electrons and holes find each other to form electron–hole pairs[3]. As both η_1 and $\eta_3 < 1$, it follows that $\eta_{EL} < \eta_2 = \eta_{max}$. Although $\sigma_S > \sigma_T$ by itself does not change the magnitude of η_2 from 1/4, in the presence of competing processes, faster rates will yield higher yields. One such competing process is the spin-lattice relaxation, which at room temperature is sufficiently fast that $\eta_{max} = \sigma_S/(\sigma_S + 3\sigma_T)$ (refs 3 and 9), rather than simply the statistical probability of obtaining one singlet exciton per three triplet excitons (see Supplementary Information). Thus the study of σ_S/σ_T in organic materials also provides information about η_{max} in organic light-emitting diodes (OLEDs).

We use continuous wave (CW) photoinduced absorption (PA) and photoinduced absorption detected magnetic resonance (PADMR) techniques (see Methods and ref. 10) to measure σ_S/σ_T in various π-conjugated polymer and oligomer thin films. For illustration, we choose the case of methylated laddertype poly-(*para*-phenylene) (mLPPP; see Fig. 1a, inset for its chemical structure[11]). In Fig. 1a we show the CW PA spectrum of mLPPP at 80 K. The PA bands labelled P_1 and P_2 are the spectral signatures

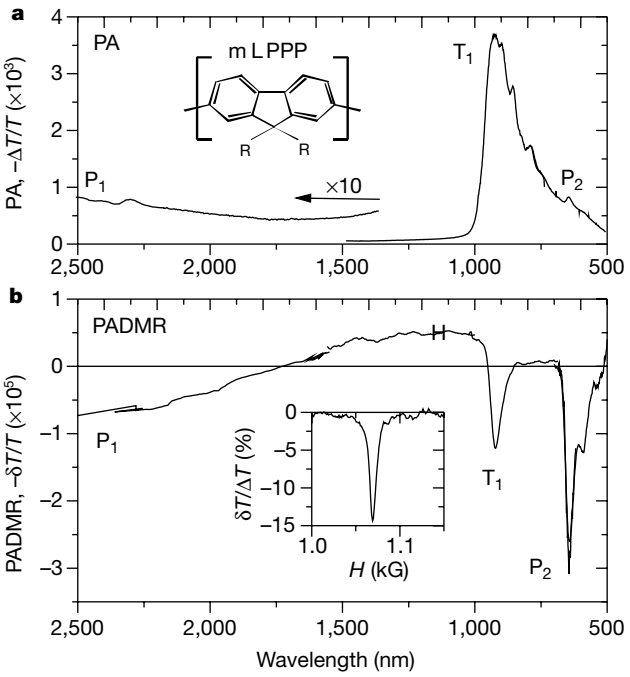

Figure 1 Spin-dependent recombination spectroscopy in π-conjugated polymers. For illustration the efficient blue emitter mLPPP (backbone is given in the inset to **a**) has been chosen. Its sharp spectral features make it ideal for spectroscopic studies[10]. **a**, The photoinduced absorption (PA) spectrum; **b**, the PA-detected magnetic resonance (PADMR) spectrum at constant magnetic field $H_{1/2} = 1.06$ kG. Both spectra **a** and **b** show two bands (P_1 and P_2) due to polarons, and one band (T_1) due to triplet absorption. The PA was measured at 80 K, the excitation was at the 457 nm line (~500 mW) of an Ar^+ laser; the PADMR spectrum was measured at 20 K. The inset in **b** shows the spin-half PADMR magnetic resonance at $H_{1/2} = 1.06$ kG detected at $\lambda = 2$ μm.

of polarons, whereas the PA band labelled T_1 corresponds to the triplet exciton[12]. Under CW illumination conditions CT reactions occur between neighbouring P^+ and P^-. The CT reaction rate R_P between spin parallel pairs (both ⇈ and ⇊), is proportional to $2\sigma_T$, whereas the reaction rate R_{AP} between spin antiparallel pairs (both ⇅ and ⇵), is proportional to $(\sigma_S + \sigma_T)$, where the proportionality constant is the same in both cases. $\sigma_S > \sigma_T$, so $R_{AP} > R_P$, and spin polarization of the recombining polaron pairs is built up over time, such that spin parallel pairs prevail under steady state illumination conditions[10].

Under saturated magnetic resonance conditions the Zeeman levels become equally populated, so that the pair densities with parallel and antiparallel spins are equal. Thus the effect of saturated magnetic resonance conditions is to increase the relative concentration of pairs with antiparallel spins whose reaction cross-section is larger, and as a consequence there is an overall decrease, δN, in the polaron population, N (see Fig. 1b inset). Figure 1b shows the wavelength-dependent PADMR spectrum of mLPPP where, in addition to a decrease in the polaron population (P_1 and P_2), a decrease in the triplet exciton population (T_1) is also measured. The negative triplet PADMR band confirms our statement that spin-half magnetic resonance decreases the population of neighbouring polaron pairs, especially those with parallel spins. The quantity $\delta T/\Delta T$ (see Methods) is then a direct measure of the fractional change in the overall photogenerated polaron population, $\delta N/N$.

The quantitative expression for $\delta N/N$ for distant pair kinetics under saturation conditions is given by[10]:

$$\delta N/N = -(R_P - R_{AP})^2/(R_P + R_{AP})^2 \qquad (1)$$

From equation (1) and the proportionality relations above between R_P, R_{AP} and σ_S, σ_T, we obtain:

$$\frac{\sigma_S}{\sigma_T} = \frac{1 + 3|\delta T/\Delta T|^{1/2}}{1 - |\delta T/\Delta T|^{1/2}} \qquad (2)$$

Thus the combination of PA and spin-half PADMR spectroscopy gives a direct measure of σ_S/σ_T. From Fig. 1b we get $\delta T/\Delta T \approx 14\%$ in mLPPP, corresponding to $\sigma_S/\sigma_T \approx 3.4$ from equation (2).

We performed similar PA and PADMR measurements for a large variety of π-conjugated polymers and oligomers. Our results are summarized in Fig. 2, where we plot the experimentally determined σ_S/σ_T as a function of the optical gap, E_g (see Supplementary Information for the experimental $\delta T/\Delta T$ values for each polymer). Individual $\sigma_S/\sigma_T > 1$ in all cases, giving $\eta_{max} > 25\%$; but there is a very large variation between the materials, which has never been seen before, to our knowledge. $\sigma_S/\sigma_T \approx 2.2$ in poly(phenylene-vinylene) (PPV), which corresponds to η_{max} of 42%, in excellent agreement with refs 2 and 9, works in which η_{max} was directly measured from OLED operation.

Although disorder, morphology and chain length distributions are all important, the systematic behaviour in Fig. 2 precludes any of these from being the dominant factor. The single biggest difference between the materials shown originates from the relative contribution of electron correlation and topology to the overall optical gap. Importantly, the lowest-energy excitations of all such systems can be mapped onto those of linear polyene chains with artificially large bond alternations[13]. We therefore theoretically examine the CT reaction between two charged polyene chains as a function of varying bond alternation.

Our goal is to calculate σ_S/σ_T for the CT reaction $|P^+\rangle + |P^-\rangle \rightarrow |[S/T]\rangle + |G\rangle$, for the case of antiparallel spins. We consider two parallel polyene chains separated by about 4 Å (Fig. 3 inset), described by the hamiltonian $H = H_1 + H_2 + H_{12}$, where H_k ($k = 1, 2$) describe the individual chains and H_{12} is the interaction between them. H_k is the single-chain Pariser–Parr–Pople hamiltonian[14,15], with the difference that the bond alternation parameter, δ, in the intrachain hopping integral[5], $t_\parallel(1 \pm \delta)$, is considered as a continuous variable. The interchain interaction is written as

$$H_{12} = \frac{1}{2}\sum_{i,j'} V_{i,j'}(n_i - 1)(n_{j'} - 1) - t_\perp \sum_{i\sigma}(c^\dagger_{i,\sigma}c_{i',\sigma} + \text{h.c.}) + \sum_{i,i',\sigma}[ii|ii'](n_i + n_{i'})(c^\dagger_{i,\sigma}c_{i',\sigma} + \text{h.c.}) \qquad (3)$$

where h.c. is hermitian conjugate. Here i (j') are carbon atoms on chain 1 (2), $c^\dagger_{i,\sigma}$ creates a π-electron of spin σ on carbon atom i, n_i is the total number of electrons on carbon atom i, $V_{i,j'}$ is the interchain Coulomb interaction, i, i' are the nearest interchain neighbours with $t_\perp$ the corresponding hopping integral (see Fig. 3 inset), and $[ii,ii']$ is the bond-charge repulsion[16]. The second and the third terms in equation (3) promote interchain CT. Here $t_\parallel$ ($t_\perp$) is the intrachain (interchain) or parallel (perpendicular) hopping integral.

Exact calculations (see Methods of relative singlet and triplet yields were performed for pairs of ethylene, butadiene and hexatriene. Calculations for such small systems are not expected to give a quantitatively valid picture, which is not possible anyway, given the uncertainties in the parameters of H_{12}. Nevertheless, we believe that it is far more important to consider the full effects of electron correlation, rather than perform approximate calculations for longer polyenes and oligomers of the experimental systems that do not capture the many-body nature of $|P^\pm\rangle$, $|S\rangle$ and $|T\rangle$. In Fig. 3 we show the results of our model calculation for two hexatriene chains, where the calculated σ_S/σ_T ratio has been plotted versus the bond alternation parameter δ, for the specific case of $t_\perp = [ii|ii'] = 0.1$ eV. The calculated σ_S/σ_T in Fig. 3 exhibits three distinct peaks, with the first (relatively small) occurring at $\delta = 0$. Qualitatively similar results were also obtained with butadiene (see Supplementary Information).

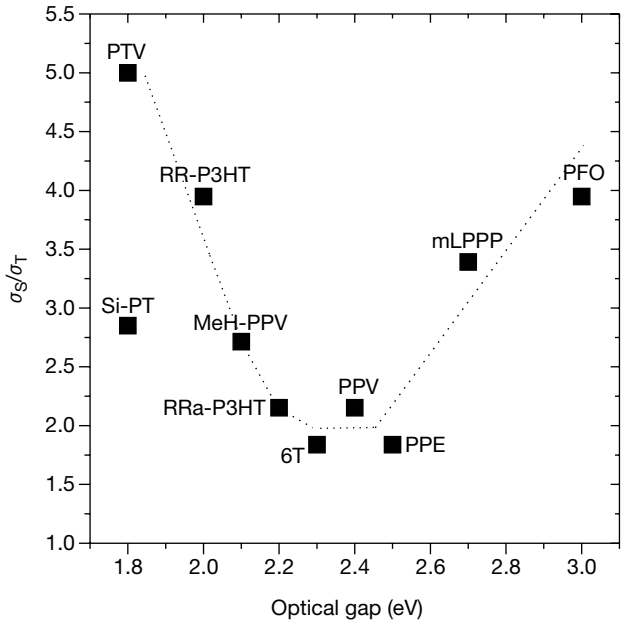

Figure 2 The experimentally determined σ_S/σ_T ratio for several π-conjugated polymers and oligomers as a function of the optical gap, E_g. σ_S/σ_T was evaluated using equation (2) from the measured $\delta T/\Delta T$ ratio for polarons in the PADMR and PA spectra, respectively. The dotted line is a guide to the eye. To ensure that δT were measured at saturated microwave absorption condition, we verified that the microwave field may be attenuated by 5 dB without reducing the observed $\delta T/\Delta T$ signals (see Supplementary Information). The values of $\delta T/\Delta T$ do not change with laser intensity or modulation frequency (see Supplementary Information) and are thus an intrinsic property of the individual polymer material.

The underlying mechanism for the occurrence of multiple peaks in Fig. 3 is as follows. For non-zero electron correlations the CT process need not lead to the lowest singlet or triplet exciton level. The correlated $|P^{\pm}\rangle$ wavefunctions, which consist of numerous configurations, change with increasing δ, and so both the individual $|EC_j\rangle$ and the specific eigenstate j that dominates the CT process evolve continuously. As a consequence of the changing character of $|P^{\pm}\rangle$, different n^1B_u exciton states dominate the CT yields at different δ, where n is the exciton quantum number. Furthermore, because the spectrum of our finite system is discrete, there exist regions of δ where neither of the two consecutive n^1B_u and $(n+1)^1B_u$ excitons give large yields. The three peaks in Fig. 3 at $\delta = 0$, 0.2 and 0.6 spectroscopically correspond to the 1^1B_u, the 2^1B_u and the 3^1B_u states, respectively (see Supplementary Information).

Similar effects also occur in the polymers (Fig. 2), where topological one-electron contributions to E_g increase from polyfluorene (PFO) to poly(thienylene vinylene) (PTV). Two aspects of the polymers allow direct comparison to our short-chain calculations. First, enhanced contribution of the topological gap to E_g can be simulated by increasing δ within effective linear-chain models[13]. Second, long-range Coulomb interactions in the Pariser–Part–Pople hamiltonian[14,15] give several excitons even in the long-chain limit[17]. Thus the qualitative effect of increased topological contribution to the optical gap is the same as increasing δ in our model calculation in Fig. 3, that is, the dominant CT product for large topological gap is a n^1B_u exciton state with n larger than 1. Experimentally, the initial ^1B_u state that is the product of the CT reaction in mLPPP and PFO has a quantum number that is larger than the initial ^1B_u state in the case of PTV and regio-regular poly(3-hexylthiophene) (RR-P3HT), with α-hexathiophene (6-HT), PPV and poly(phenylene-ethylene) (PPE) lying in a region of parameter space that corresponds to one of the valleys in Fig. 3. It is difficult to assign δ values to all systems in Fig. 2. Previous work has assigned $\delta \geqslant 0.2$ to PPV (ref. 13), and with moderate shifts of the peaks in Fig. 3 with chain length to lower δ (see Supplementary Information), the valley in σ_S/σ_T may well occur near $\delta \simeq 0.2$, with the next peak occurring at $\delta \approx 0.5$. We therefore conclude that the obtained systematic variation of the σ_S/σ_T shown in Fig. 2 is a distinct signature of the excitonic energy spectrum of the lowest-lying excited states in π-conjugated polymers.

We have thus discovered, to the best of our knowledge, a new experimental technique to determine the σ_S/σ_T ratio in π-conjugated polymers and oligomers using a spin-dependent recombination spectroscopy. The technique is very general, and may be used in other organic or inorganic materials that have long-lived charge excitations, particularly in determining the maximum EL yield in OLEDs made from the individual systems. Theoretically, our approach takes into account the full effects of electron correlation. The curious variation obtained in σ_S/σ_T with E_g is a novel electron correlation effect, that gives a new perspective on the electron–hole recombination in organic semiconductors. □

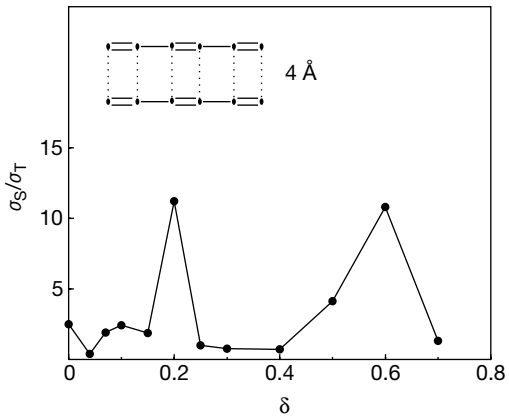

Figure 3 The calculated σ_S/σ_T for two parallel chains of hexatriene as a function of hypothetical bond alternation δ. The inset shows the actual arrangement of the chains chosen for the calculation.

Methods

The CW PA and spin-half PADMR techniques

The CW PA technique measures the excited state absorption spectrum of long-lived photoexcitations, such as triplet excitons and charged polarons. Two light beams are used; for the excitation beam we used an Ar^+ laser, the intensity of which was modulated with a chopper. We measured the pump-beam-induced changes, ΔT, in the probe beam (tungsten halogen lamp) transmission, T, using a monochromator and a combination of solid state detectors. The concentration, N, of the long-lived species is proportional to the corresponding PA intensity ($-\Delta T/T$).

The PADMR technique measures the effect of spin-half magnetic resonance on the steady state population of photogenerated polarons and triplets. The experiment consists, in addition to the PA set-up, of a magnetic resonance part (microwave source and resonator, superconducting magnet). The sample is put inside the resonator and cooled by liquid helium. The PADMR set-up allows both PA and PADMR measurements under identical conditions. The change, δN, in the steady state population is proportional to the corresponding PADMR intensity ($-\delta T.T$, where δT is the resonant change in transmission). Experimentally the PADMR resonance is achieved by matching the energy splitting between the two Zeeman levels at magnetic field $H_{1/2}$ to the photon energy of an intense microwave field. For the 3-GHz microwave resonator used here, $H_{1/2}$ (corresponding to a g-value of 2) amounts to 1,060 G.

Computational technique

The approach for calculating σ_S/σ_T for the two charge chains is as follows. We use a time-dependent Schrödinger approach to calculate the time evolution of the initial state $\psi(0) = |P^+\rangle|P^-\rangle$, when operated by the overall hamiltonian H. The time evolution is done following a discretized procedure (see Supplementary Information), and after each evolution step, the evolved state $\psi(t)$ (which contains all the $|EC_j\rangle$) is projected onto the product of the eigenstates of the neutral systems. The yield for a given pair of product states is the overlap $|\langle\psi(t)|m,n\rangle|^2$, where $|m,n\rangle = |m\rangle \times |n\rangle$, with one of the two components $|m\rangle$ and $|n\rangle$ corresponding to $|[S/T]\rangle$ and the other to $|G\rangle$. The procedure was checked by performing the calculations first for the one-electron limit, where all yields are known.

Received 21 September; accepted 5 December 2000.

1. Friend, R. H. *et al.* Electroluminescence in conjugated polymers. *Nature* **397,** 121–128 (1999).
2. Cao, Y., Parker, I. D., Yu, G., Zhang, C. & Heeger, A. J. Improved quantum efficiency for electroluminescence in semiconducting polymers. *Nature* **397,** 414–417 (1999).
3. Shuai, Z., Beljonne, D., Silbey, R. J. & Bredas, J. L. Singlet and triplet exciton formation rates in conjugated polymer light-emitting diodes. *Phys. Rev. Lett.* **84,** 131–134 (2000).
4. Campbell, D. K., Bishop, A. R. & Fesser, K. Polarons in quasi-one-dimensional systems. *Phys. Rev. B* **26,** 6862–6874 (1982).
5. Soos, Z. G. & Ramasesha, S. Valence bond theory of linear Hubbard and Pariser-Parr-Pople models. *Phys. Rev. B* **29,** 5410–5422 (1984).
6. Lavrentiev, M. Yu., Barford, W., Martin, S. J., Daly, H. & Bursill, R. J. Theoretical investigation of the low-lying electronic structure of poly(p-phenylene vinylene). *Phys. Rev. B* **59,** 9987–9994 (1999).
7. Rohlfing, M. & Louie, S. G. Optical excitations in conjugated polymers. *Phys. Rev. Lett.* **82,** 1959–1962 (1999).
8. Monkman, A. P. *et al.* The triplet state of the ladder-type methyl-poly(p-phenylene) as seen by pulse radiolysis-energy transfer. *Chem. Phys. Lett.* **327,** 111–116 (2000).
9. Kim, J., Ho, P. K. H., Greenham, N. C. & Friend, R. H. Electroluminescence emission pattern of organic light-emitting diodes: Implications for device efficiency calculations. *J. Appl. Phys.* **88,** 1073–1081 (2000).
10. Vardeny, Z. V. & Wei, X. in *Handbook of Conducting Polymers II* (eds Skotheim, T. A., Elsenbaumer, R. L. & Reynolds, J. R.) 639–666 (Marcel Dekker, New York, 1997).
11. Graupner, W. *et al.* Direct observation of ultrafast field-induced charge generation in ladder-type poly(para-phenylene). *Phys. Rev. Lett.* **81,** 3259–3262 (1998).
12. Wohlgenannt, M., Graupner, W., Leising, G. & Vardeny, Z. V. Photogeneration and recombination processes of neutral and charged excitations in films of a ladder-type poly(para-phenylene). *Phys. Rev. B* **60,** 5321–5330 (1999).
13. Soos, Z. G., Ramasesha, S. & Galvão, D. S. Band to correlated crossover in alternating Hubbard and Pariser-Parr-Pople chains: Nature of the lowest singlet excitation of conjugated polymers. *Phys. Rev. Lett.* **71,** 1609–1612 (1993).
14. Pariser, R. & Parr, R. G. A semi-empirical theory of the electronic spectra and electronic structure of complex unsaturated molecules II. *J. Chem. Phys.* **21,** 767–776 (1953).
15. Pople, J. A. Electron interaction in unsaturated hydrocarbons. *Trans. Faraday Soc.* **49,** 1375–1385 (1953).
16. Campbell, D. K., Gammel, J. T. & Loh, E. Y. Bond-charge Coulomb repulsion in Peierls-Hubbard models. *Phys. Rev. B* **38,** 12043–12046 (1988).
17. Gallagher, F. & Mazumdar, S. Excitons and optical absorption in one-dimensional extended Hubbard models with short- and long-range interactions. *Phys. Rev. B* **56,** 15025–15039 (1997).

Supplementary information is available on *Nature*'s World-Wide Web site or as paper copy from the London editorial office of *Nature*.

Acknowledgements

We thank E.J.W. List for supplying the mLPPP polymer, and X.M. Jiang and E.J.W. List for their support in performing the experiments. The work at the University of Utah was supported in part by the DOE and the NSF. Work in Arizona was partially supported by the ONR through the MURI centre (CAMP) at the University of Arizona. Work in Bangalor was funded by CSIR, India.

Correspondence and requests for materials should be addressed to Z.V.V. (e-mail: val@physics.utah.edu).